Available online at www.sciencedirect.com

ScienceDirect

Procedia CIRP 101 (2021) 142–145

www.elsevier.com/locate/procedia

9th CIRP Conference on High Performance Cutting (HPC 2020)

Regenerative instabilities of spring-guided circular saws

Sunny Singhania[a], Mohit Law[a,*]

[a]*Machine Tool Dynamics Laboratory, Department of Mechanical Engineering, Indian Institute of Technology Kanpur, Kanpur 208016, India.*

* Corresponding author. Tel.: +91-512-679-6897; fax: +91-512-679-7408. *E-mail address:* mlaw@iitk.ac.in

Abstract

This paper presents analytical model-based analysis of the stability of spring-guided rotating and flexible circular saws subjected to regenerative lateral cutting forces. The saw is modelled as an annular circular plate constrained by a guide modelled as a point spring. The governing equation of motion accounts for inertial, gyroscopic, and stiffness terms, and the time-dependent periodic forces generated by the saw-workpiece interaction. Stability analysis for different materials and engagements show regenerative instabilities to be influenced by the guide, and critical speed related instabilities to not change with the guide. Results are instructive to guide the design of stable sawing processes.

Keywords: Stability; Vibration; Circular sawing

1. Introduction

The circular sawing process involves feeding a rotating saw into a workpiece to cut it to sections of required lengths and/or widths. The process is common across the wood working and metal cutting industries. To keep kerf losses at a minimum, the saws are usually thin. Their thinness makes them flexible and prone to vibration borne critical speed related instabilities, and to regenerative instabilities. Critical speed related instabilities occur when the rotational speed of the saw corresponds to one of its natural frequencies. Regenerative instabilities on the other hand occur due to sawing process induced self-excited vibrations. Large amplitude vibrations resulting from these instabilities can damage the saw, machine, and the workpiece, There has hence been sustained research effort to understand and mitigate the mechanisms responsible for these instabilities.

Even though both instabilities are known to occur in circular sawing, the emphasis has been more towards understanding and mitigating critical speed related instabilities [1–9], and correspondingly less research attention has been paid on the modelling and mitigation of regenerative instabilities, the notable exception being the work reported in [10-11]. Furthermore, most reported work on circular sawing has been for the wood cutting application that is performed at higher speeds, and that is limited more by critical speed related instabilities than regenerative instabilities. This paper, however, is more concerned with circular sawing for metal cutting than for wood, and since metal cutting operations are performed at relatively lower speeds than the speeds at which wood is cut, it is important to understand which of the two instabilities kicks in first, such that it can be mitigated appropriately. This is indeed one of the aims of this paper.

Modelling the dynamics and stability of circular saws, whether idling [1], and/or under the influence of concentrated radial, tangential, and lateral forces [2–3] has been studied extensively. There has also been sustained interest in understanding the role of guides in constraining the lateral motion of saws, and also their role in stabilizing and increasing the critical speeds [4–10]. Since these guides offer resistance to motion, and act as a transverse load, how/if their presence influences regenerative instabilities is yet unknown. Addressing this question is another aim of the present paper.

The present study builds on our dynamic and critical speed stability models reported earlier [9] and considers a cutting

10.1016/j.procir.2021.02.017

force model involving multiple moving concentrated cutting forces over a given space-fixed sector to investigate the regenerative stability characteristics. We build on the regenerative model discussed in [10-12]. We also expand the model in [10–11] by including the influence of a guide modelled as a point spring. Furthermore, since circular sawing is essentially a milling operation, there will be three components of forces acting on every cutting tooth, and, in general over a space-fixed sector, and even though the primary forces might be the in-plane tangential and radial cutting forces, since the saw is more flexible in the lateral direction than in its in-plane directions, this paper will only factor the influence of the lateral regenerative cutting force on the stability of the system, while ignoring the contributions of the in-plane forces.

The remainder of the paper is organized as follows: Section 2 presents the expanded analytical model for the dynamics and stability of a spring-guided circular saw that includes lateral regenerative forces. Section 3 presents analytical model-based investigations on the influence of the guide on critical speeds and regeneration related instabilities. This section includes discussions on the stability of the process for cutting different materials, and for cutting with different engagement conditions. The paper is finally concluded in Section 4.

2. Analytical model of instabilities of a spring-guided circular saw

A circular saw made of steel (E = 208 GPa, ρ = 7850 kg/m^3, ν = 0.3), and with 60 teeth, (N_t = 60), and that is laterally constrained by a guide pad modelled as a point spring is shown in Fig. 1. The saw is modelled as an annular circular plate with a clamped inner radius, r_i = 42.5 mm, and a free outer radius, r_o = 142.5 mm, and a thickness, h = 2 mm, rotating with an angular velocity of Ω in the clockwise direction. The saw is assumed to be cutting a solid bar of some material with a diameter 76 mm. The instantaneous entry angle of the saw in the cut, θ_{st} and the corresponding exit angle, θ_{ex} are as shown in the Fig 1. The point spring with stiffness, k_g is located at r_m, θ_m as shown and applies a point force of q on the saw.

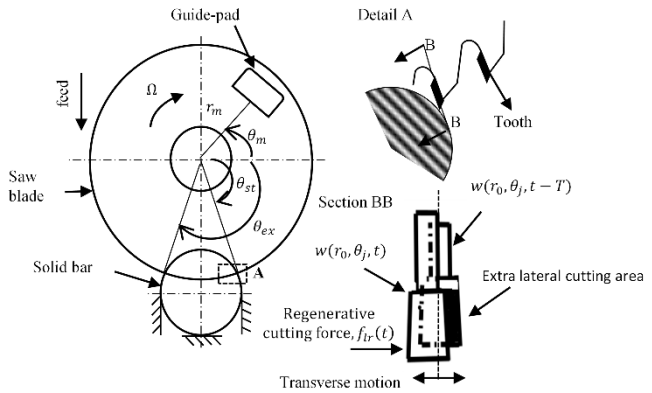

Fig. 1. Schematic showing a guided circular saw cutting a solid bar and subjected to lateral regenerative cutting forces

Our model, like the model we base our investigations on [10 – 11], assumes that the saw is only flexible in the lateral direction. Neglecting the in-plane radial and tangential forces, and assuming that only the lateral component of the cutting force ($f_{lr}(t)$) makes the saw oscillate laterally, and that the cutting force is always normal to the undeformed plane of the saw, there is an extra lateral cutting area between two successive teeth associated with the transverse response $w(r_o, \theta_j, t)$ of the current tooth (the jth tooth) and the transverse response $w(r_o, \theta_j, t-T)$ of the previous tooth (the (j-1) th tooth) at a given location (r_o, θ_j) of the workpiece [10]. $T = 2\pi/\Omega N_t$ is the tooth passing period, i.e., the period between two successive teeth coming into cut.

The modified governing equation of motion for transverse vibrations of the spring-guided circular saw subjected to a lateral regenerative cutting force and a guide force in the stationary frame of reference, and that includes the bending stiffness of the saw, the inertial stress, and the in-plane rotational stress, is given by:

$$D\nabla^4 w + \rho h\left(\frac{\partial^2 w}{\partial t^2} + 2\Omega\frac{\partial^2 w}{\partial t \partial\theta} + \Omega^2\frac{\partial^2 w}{\partial\theta^2}\right) - h\left[\left(\frac{1}{r}\right)\left(\frac{\partial}{\partial r}\right)\left(r\sigma_r\frac{\partial w}{\partial r}\right) + \left(\frac{1}{r^2}\right)\left(\frac{\partial}{\partial\theta}\right)\left(\sigma_\theta\frac{\partial w}{\partial\theta}\right)\right] = f_{lr}(t) + q, \quad (1)$$

wherein, D is the flexural rigidity (= Eh^3/ (12(1-ν^2)), and ∇^4 is the bi-harmonic operator. σ_r and σ_θ are the rotational stresses that are neglected in this preliminary analysis. The transverse force corresponding to regenerative effect and due to the guide is represented as [9 -11]:

$$f_{lr}(t) = -\sum_{j=1}^{N_t}\left(\frac{1}{r}\right)K_r[w(r,\theta,t) - w(r,\theta,t-T)]\delta(r - r_0)\delta(\theta-\theta_j)\,g(\theta_j) \quad (2)$$

$$q = -k_g w(r,\theta,t)\left(\frac{1}{r}\right)\delta(r - \mathrm{r_m})\delta(\theta-\theta_m), \quad (3)$$

wherein in Eq. (2) N_t are the total number of teeth in cut; K_r is an empirically determined cutting force coefficient that is a function of the material being cut, the cutting parameters, and the geometry of the saw tooth, and this coefficient can be mechanistically identified as discussed in [12]. $\delta(.)$ in Eq. (2) and in Eq. (3) is the Dirac delta function, and $g(\theta_j)$ is a screening function to determine if the tooth is in cut or not, i.e., $g(\theta_j) = 1$, when $\theta_{st} < \theta_j < \theta_{ex}$, and $g(\theta_j) = 0$ otherwise. The instantaneous tooth position θ_j is given by: $\theta_j = \theta_{st} + \Omega t + (j-1)\theta_p$, ($\theta_1 = \theta_{st}$ when $t = 0; \theta_p$ is the angular pitch). Substituting Eq. (2) and Eq. (3) into the governing equation of motion and applying the Galerkin projection method leads to an equation of motion of the form [10 - 11]:

$$[\boldsymbol{M}]\{\ddot{\boldsymbol{x}}\} + [\boldsymbol{G}]\{\dot{\boldsymbol{x}}\} + [\boldsymbol{K}]\{\boldsymbol{x}\} + (1 - \mathrm{e}^{-TD})[\boldsymbol{A}(\boldsymbol{t})]\{\boldsymbol{x}\} = \{\boldsymbol{0}\} \quad (4)$$

wherein $\mathrm{e}^{-TD}\{\boldsymbol{x}(\boldsymbol{t})\} = \{\boldsymbol{x}(\boldsymbol{t}-\boldsymbol{T})\}$, and $[\boldsymbol{M}]$, $[\boldsymbol{G}]$, and $[\boldsymbol{K}]$ are mass, gyroscopic and stiffness matrices. $[\boldsymbol{A}(\boldsymbol{t})]$ is a time periodic varying matrix associated with the cutting forces [13].

The solution to Eq. (4) with periodic coefficients can be assumed in the form of a Fourier series [11]:

$$\{\boldsymbol{x}(\boldsymbol{t})\} = \left[\frac{\{\boldsymbol{b_0}\}}{2} + \sum_{k=1}^{\infty}(\{\boldsymbol{a_k}\}\sin(kwt)) + \{\boldsymbol{b_k}\}\cos(kwt)\right]\mathrm{e}^{\lambda t}$$

wherein $\{\boldsymbol{b_0}\}$, $\{\boldsymbol{a_k}\}$ and $\{\boldsymbol{b_k}\}$ are time-invariant coefficient vectors, and λ is the characteristic variable of the system [11].

Since $[\boldsymbol{A}(\boldsymbol{t})]$ is also periodic, as was proposed in [13] for the case of a regenerative model for milling processes, in this case too, it can be expressed in a Fourier series form [11, 13]:

$$[\boldsymbol{A(t)}] = \left[\frac{[\boldsymbol{B_0}]}{2} + \sum_{k=1}^{\infty}([\boldsymbol{A_k}]\sin(kwt)) + [\boldsymbol{B_k}]\cos(kwt)\right].$$

Substituting the assumed solutions in Eq. (4) and equating the coefficients of $e^{\lambda t}$ on both sides, and after simplifying for the case of only taking the zeroth order approximation, the characteristic equation of the system reduces to:

$$\left(\lambda^2[\boldsymbol{M}] + \lambda[\boldsymbol{G}] + [\boldsymbol{K}] + \left(1 - e^{-T\lambda}\right)\left[\frac{\boldsymbol{B_0}}{2}\right]\right)\{\boldsymbol{b_0}\} = \{\boldsymbol{0}\}. \quad (5)$$

The roots of this characteristic equation can be solved to determine the stability of this system. However, to do so, we first assume that the transverse deflection for the circular saw for the special case of a single-mode solution can be approximated as follows [11]:

$$w(r,\theta,t) = R_{mn}(r)[\boldsymbol{C_{mn}(t)}\cos(n\theta) + \boldsymbol{S_{mn}(t)}\sin(n\theta)] \quad (6)$$

wherein $R_{mn}(r)$ satisfies the saw boundary conditions of the saw being clamped at its inner section and free at its periphery; and m and n correspond to the nodal circle and nodal diameters of interest. Substituting Eq. (6) in Eq. (1), and again applying the Galerkin procedure leads to a similar form of Eq. (4), wherein, it can be shown that [11]:

$$\left.\begin{aligned}[\boldsymbol{A(t)}] &= \textstyle\sum_{j=1}^{N_t} g(\theta_j)\left[\boldsymbol{P(\theta_j)}\right];\\ \left[\boldsymbol{P(\theta_j)}\right] &= R_{mn}^2(r_0)\begin{bmatrix} K_r\cos^2(n\theta_j) & K_r\sin(\frac{2n\theta_j}{2}) \\ K_r\sin(\frac{2n\theta_j}{2}) & K_r\sin^2(n\theta_j)\end{bmatrix};\\ [\boldsymbol{B_0}] &= \tfrac{2}{T}\textstyle\int_0^T[\boldsymbol{A(t)}]\,dt \equiv \frac{N_t}{\pi}\int_{\theta_{st}}^{\theta_{ex}}\left[\boldsymbol{P(\theta_j)}\right]d\theta\end{aligned}\right\}. \quad (7)$$

Substitution of Eq. (7) into the characteristic Eq. (5) and using the Muller's optimization algorithm [11, 14] with deflation to solve the resulting complex nonlinear equations yields the eigenvalues of the system for every speed of interest. The resulting eigenvalues at every speed are complex valued, i.e., $\lambda = \alpha + i\omega$, wherein the imaginary part corresponds to the natural frequency of the system, and the real part corresponds to the growth.

Having described the analytical model for the stability of the spring-guided circular saw subjected to regenerative lateral cutting forces, we now present numerical analysis of the influence of the guide on critical speed related instability as well as regenerative instability – as is discussed next.

3. Numerical results and discussions

This section discusses how instabilities are influenced by the introduction of a guide. At first, in Section 3.1, instabilities are compared for cutting a specific material characterized by a fixed cutting force coefficient, and for the instantaneous cutting at a fixed engagement condition. This is followed in Section 3.2 with discussions on how the material being cut can potentially change instabilities. And, Section 3.3 discusses the instabilities changing with changing engagement conditions.

All analysis presented herein is limited to the single mode case i.e., for the $m = 0, n = 2$ mode. Furthermore, for all analysis herein, the guide is assumed to be placed at a radial location of $r_m = 0.14$ m, and with an orientation of $\theta_m = 30^0$. The spring stiffness of the guide is assumed to fixed at $k_g = 10^5$ N/m.

3.1. Critical speeds and regenerative instabilities of the guided circular saw

Assuming that the material being cut can be characterized by a cutting force coefficient of $K_r = 10$ N/m, and considering the engagement conditions to be fixed at entry and exit angles of $\theta_{st} = 73^0$ and $\theta_{ex} = 107^0$ respectively, the resulting loci of the imaginary and real parts of the eigenvalues are shown in Fig. 2 for the case with and without the guide.

As is evident from Fig. 2(a), the critical speeds, i.e., the speeds (or correspondingly the tooth passing frequencies, i.e., $(\omega_n/2\pi) \times (N_t/60)$) at which the natural frequencies of the backward travelling waves becomes zero, remains the same for the case of a spring-guided circular saw subjected to lateral regenerative instabilities, as it does for the saw without a guide and with regenerative effects considered. These results are consistent with what was reported on earlier, even for the case without regenerative effects included [7, 9]. Furthermore, even though the critical speed remains unchanged, introduction of the guide splits the mode at zero speeds, and also changes the characteristic behavior of the Campbell diagram – which is also consistent with earlier reported results which did not include the regenerative effects [7, 9].

Interestingly however, even though the critical speed remains unchanged, the regions of regenerative instabilities (i.e., the regions for which the real part of the eigenvalue is positive) for a guided saw are very different than the saw that is not guided – as is evident from Fig. 2(b). It is also evident that both the forward and backward waves can cause regenerative instabilities, as opposed to the critical speed being governed by only the backward wave. It is further evident that regenerative instabilities occur at much lower speeds as compared with the critical speed. And, since this paper is more interested in the circular sawing of metal that takes place at lower speeds, the regenerative instabilities are of more interest to us than the critical speed related instabilities, and as such results in the subsequent sections are limited to only discussing regenerative instabilities for lower tooth passing frequencies.

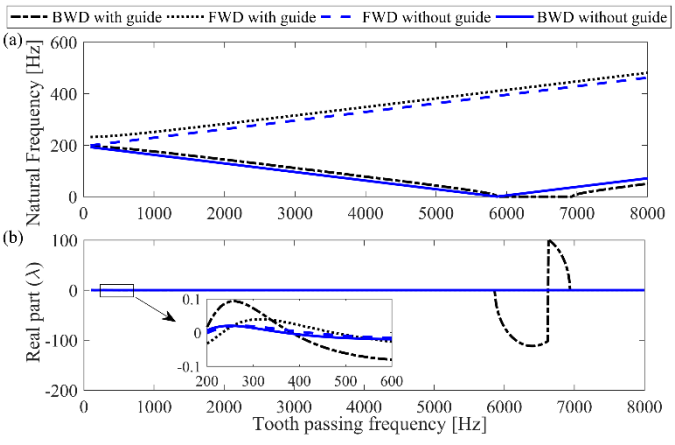

Fig. 2. Comparison of natural frequencies (a), and real parts of λ (b) for a saw that is guided and not. (BWD- backward wave, FWD- Forward wave).

3.2. Regenerative instabilities of the guided circular saw for different materials

Keeping all things the same as in the Section 3.1, regenerative instabilities were investigated for the case of the guided saw by changing only the material dependent cutting force coefficient, K_r. The low level of K_r = 10 N/m corresponds to cutting a soft material, and the high level of K_r = 1000 N/m, corresponds to cutting a relatively more difficult-to-cut material. Results for these are shown in Fig. 3, and, as is evident, an increase in K_r does not change the region of instability, and only changes the rate of growth of the instability. These results are consistent with those reported in [10 - 11], even though those results were reported for the saw not being guided.

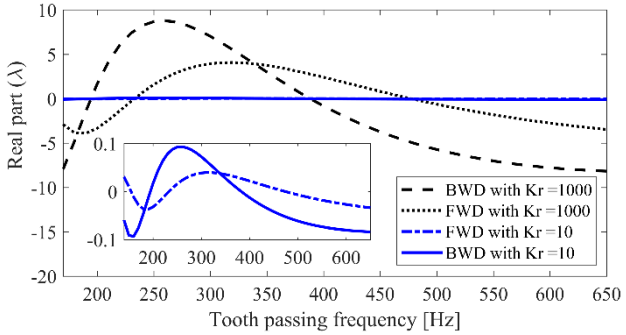

Fig. 3. Comparison of regenerative instabilities for different workpiece materials (BWD- backward wave, FWD-forward wave).

3.3. Regenerative instabilities of the guided circular saw for different engagement conditions

As the saw progress in the cut, the engagement conditions, and the active number of teeth in cut change. Regenerative instabilities were hence investigated with two different engagement conditions, one low ($\theta_{st} = 80^0$ and $\theta_{ex} = 100^0$) and one relatively higher ($\theta_{st} = 73^0$ and $\theta_{ex} = 107^0$), with correspondingly low ($N_t = 4$) and high ($N_t = 6$) levels of active teeth in cut. Results herein are limited to cutting a material with a higher cutting force coefficient of 1000 N/m.

Results shown in Fig. 4 make clear that the regions of instabilities do not change with changing engagement conditions, or with the change in the active number of teeth in cut, and only the rate of growth of the instability increases with larger engagements and with more number of active teeth in cut. These results are also consistent with observations made in [10 - 11], even though those results were for an unguided saw.

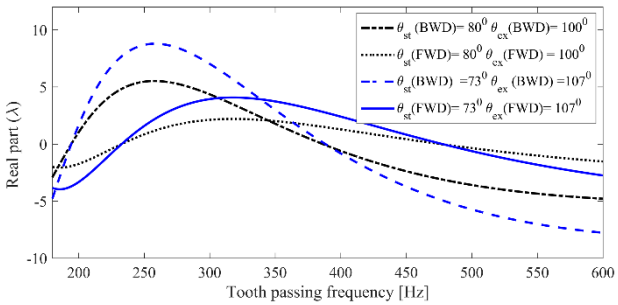

Fig. 4. Comparison of regenerative instabilities for different engagement conditions (BWD- backward wave, FWD-forward wave).

4. Conclusions and outlook

The critical speed related instabilities and regenerative instabilities for a guided circular saw were investigated in this paper. An expanded analytical model that described the guide as a single point spring and accounted for the regenerative lateral cutting forces was presented.

Numerical simulations for a single mode revealed that the critical speed for a single spring-guided circular saw remains unchanged from the case of the saw that is not guided. Investigations also revealed that regenerative instabilities occur well below the critical speed, and that the regenerative instabilities are influenced by the saw being guided. Investigations also reveal that the intensity of the regenerative instability is governed by the material being cut, and by the engagement conditions and the number of active teeth in cut. Since circular saws are usually guided, the models and results presented herein can help instruct the placement of guides and in selection of guide material and cutting parameters that may stabilize circular sawing.

Further research is necessary to understand the stability with multiple guides for the multi-mode case, and potentially with multiple regenerations taking place in multiple directions. The influence of the mass, damping and friction induced by the guide also must be addressed appropriately, as should the potential influence of any in-plane regenerative forces on the stability of the system.

Acknowledgements

This research was supported by the Government of India's Science and Engineering Research Board's Early Career Research Award – SERB/ECR/2016/000619.

References

[1] Mote C.D., Nieh L. T. On the foundation of circular-saw stability theory. Wood Fiber Science 1973; 5(2): 160–169.
[2] Radcliffe C.J., Mote C.D. Stability of stationary and rotating discs under edge load. International Journal of Mechanical Science 1977; 19: 567-574.
[3] Chonan S, Jiang Z.W., Yuki Y, Vibration and deflection of a silicon-wafer slicer cutting the crystal ingot J. Vib. Acoust. 1993;115(4):529-34.
[4] Iwan W. D, Moeller T. L, The stability of a spinning elastic disk with a transverse load system. J. Appl. Mech 1976; 43(3): 485–490.
[5] Hutton S.G., Chonan S, Lehmann B.F, Dynamic response of a guided circular saw. J. Sound Vib.1987; 112(3): 527–539.
[6] Lehmann B.F., Hutton S.G, Self-excitation in guided circular saws. J. Vib. Acoust. 1988; 110(3): 338–344.
[7] Schajer G.S., Guided circular saw critical speed theory.Proc. saw tech 1989.
[8] Mohammadpanah A., Hutton S.G., Flutter instability speeds of guided splined disks. Shock Vibration 2015; 2015.
[9] Singhania S, Kumar P, Gupta S. K., Law M., Influence of guides on critical speeds of circular saws. Adv. in Comp. Methods in Mfg. 2019.
[10] Tian J.F., Hutton S.G., Self-excitation in flexible rotating discs subjected to various transverse interactive forces. ASME J. Appl. Mech. 1999; 66.
[11] Tian J.F., Hutton S.G., Cutting-induced vibration in circular saws. J. Sound Vib. 2001; 242(5): 907-922.
[12] Altintas Y., Manufacturing automation Cambridge university press; 2012.
[13] Altintas Y., Budak E., Analytical prediction of stability lobes in milling. CIRP annals. 1995; 44(1):357-62.
[14] Mathews J.H, Numerical Methods for Mathematics, Science and Engg.